IMPLANT SURFACES AND INTERFACE PROCESSES

B. KASEMO
J. GOLD

Department of Applied Physics
Chalmers University of Technology and
Göteborg University
412 96 Göteborg, Sweden

Adv Dent Res 13:8-20, June, 1999

Abstract—The past decades and current R&D of biomaterials and medical implants show some general trends. One major trend is an increased degree of functionalization of the material surface, better to meet the demands of the biological host system. While the biomaterials of the past and those in current use are essentially bulk materials (metals, ceramics, polymers) or special compounds (bioglasses), possibly with some additional coating (*e.g.*, hydroxyapatite), the current R&D on surface modifications points toward much more complex and multifunctional surfaces for the future. Such surface modifications can be divided into three classes, one aiming toward an optimized three-dimensional *physical micro-architecture* of the surface (pore size distributions, "roughness", etc.), the second one focusing on the (bio) *chemical properties* of surface coatings and impregnations (ion release, multi-layer coatings, coatings with biomolecules, controlled drug release, etc.), and the third one dealing with the *viscoelastic properties* (or more generally the micromechanical properties) of material surfaces. These properties are expected to affect the interfacial processes cooperatively, *i.e.*, there are likely synergistic effects between and among them: The surface is "recognized" by the biological system through the combined chemical and topographic pattern of the surface, and the viscoelastic properties. In this presentation, the development indicated above is discussed briefly, and current R&D in this area is illustrated with a number of examples from our own research. The latter include micro- and nanofabrication of surface patterns and topographies by the use of laser machining, photolithographic techniques, and electron beam and colloidal lithographies to produce controlled structures on implant surfaces in the size range 10 nm to 100 μm. Examples of biochemical modifications include mono- or lipid membranes and protein coatings on different surfaces. A new method to evaluate, *e.g.*, biomaterial-protein and biomaterial-cell interactions—the Quartz Crystal Microbalance—is described briefly.

Key words: Surface topography, surface chemistry, lithography, lipid membranes, protein coatings, quartz crystal microbalance.

Presented at the 15th International Conference on Oral Biology (ICOB), "Oral Biology and Dental Implants", held in Baveno, Italy, June 28-July 1, 1998, sponsored by the International Association for Dental Research and supported by Unilever Dental Research

The first paper one of us wrote in the area of biomaterials had the title "Biocompatibility of titanium implants—Surface science aspects" (Kasemo, 1983). It collected some early ideas and working hypotheses that had emerged from stimulating discussions with professor P.-I. Brånemark and his team (Albrektsson *et al.*, 1983). These ideas were further articulated in a longer paper in 1985 (Kasemo and Lausmaa, 1985).

What were the main questions addressed at that time—some 15-20 years ago—and what were the general views on the role of surfaces in the area of medical implants? Major questions were: Were surface properties important at all? Did details like surface purity, contamination, etc., play any role? and Was surface roughness/topography important? This subset of questions belonged to a larger set, dealing with the general biology and clinical aspects of the implant-tissue interface.

The driving forces for the rapid research development after this time were of both purely scientific origin, driven by investigators' desire to understand the basic processes occurring at the implant-tissue interface, and of practical (clinical and industrial) origin. The clinical goal was, of course, to develop better, more reliable and functional implants. From a regulatory and production point of view, it was necessary to know which of the surface properties were practically important, to develop quality standards for medical implants and to establish standardized manufacturing processes.

So what has happened since the early 1980's? From a very long "possible" list, we consider the following six points to be the most important at present:

(i) A detailed, consistent, and coherent picture of the processes and major mechanisms at the interface is still lacking.

(ii) The problem formulation and the working hypotheses have matured enormously through a massive and systematic experimental research effort. For example, the question whether surface chemistry or surface topography is the most important surface property has transformed from an "either/or" question to the view that both are important and functionally coupled.

(iii) The use of surface analytical methods has become standard practice in experimental evaluations of biomaterial surfaces, in contrast to ~ 15 years ago, when they were regarded as exotic new methods of questionable value.

(iv) The quality, variety, and sophistication of surface preparations have increased enormously, including organic overlayers, topographic modifications, and impregnation with biologically active substances, etc.

(v) A large number of experimental methods and new knowledge from other fields have been brought into biomaterials research, such as scanning probe microscopies and microfabrication techniques.

(vi) The intense development in molecular biology is slowly but steadily providing biomaterials research with a whole new set of diagnostic and preparative tools.

These issues, especially in areas (ii)-(v), are further articulated in the next section. In §3, results from current research in our group are presented, illustrating some new preparative and analytical research directions for biomaterials.

(2) THE IMPLANT-TISSUE INTERFACE

Fig. 1 is an attempt to obtain a "bird's eye view" of processes and properties at the interface (adapted from Kasemo and Lausmaa, 1986). The intention is to give a pictorial and conceptual idea in the time-space domain of the interface and its evolution. To catch the many different length scales involved, the picture has two logarithmic scales: a horizontal length scale with the original implant surface at the very interface, *i.e.*, at the transition plane between the implant side (to the left) and the biological side (to the right). The finest microscopic details of atomic and molecular sizes are resolved at the very interface, while farther from the surface, only larger aggregates like cells ~ 10 μm are resolved. [Actually, this picture underlines that the most intimate details of the interface can be revealed only by microscopies with much better resolution than optical microscopy (> 0.5 μm), such as scanning electron microscopy (SEM, ~ 10 nm) or transmission electron microscopy, TEM (better than 1 nm).] The vertical scale represents time, increasing from bottom to top, also on a logarithmic scale, so that time is highly resolved at the initial period after implantation, with rapidly varying conditions at the interface, and successively less resolved at longer times, when the evolution of the interface is slower and slower. The picture schematically illustrates how the interface zone, grossly perturbed after surgery, successively re-organizes and closes the gap between the implant and the unperturbed tissue.

Let us consider, in a little more detail, the scenario at the surface, starting with an ideal clean implant surface (Fig. 2). The originally clean surface (Fig. 2a) will inevitably be contaminated (Kasemo and Lausmaa, 1988) unless very special precautions are taken. Typical contaminations are (Fig. 2b) hydrocarbons and both inorganic and organic sulphur and nitrogen compounds. Such contamination can, however, be reduced or eliminated by different cleaning and "passivation" steps (Fig. 2c). "Passivation" means a saturation of the dangling bonds of surface atoms (Kasemo and Lausmaa, 1988) and can sometimes be achieved by special treatment of the native surface, or by coating the surface with a specially designed protective overlayer.

If such a surface is implanted, its first encounter with the bioworld is with the totally dominating water molecules. They will rapidly bind to the surface, and form a water mono- or bilayer (Fig. 2d) whose structure is very different from that of liquid water (Thiel and Madey, 1987; Vogler, 1998). The specific arrangement of water molecules is sensitive, depending on the surface properties at the atomic scale. On very reactive surfaces, the H_2O molecules may dissociate and form a hydroxylated (*i.e.*, OH-terminated) surface. A second type of surface binds H_2O molecules strongly (more strongly than the H-bonded network of ice), but still as intact, non-dissociated molecules. Both these surface types are hydrophilic, *i.e.*, wetting surfaces. On a third type of surface, the H_2O-surface bond is weaker than the hydrogen bonds in ice, which is the surface type we call non-wetting or hydrophobic. Thus, the concepts of hydrophobic and hydrophilic are directly related to the binding strength of water to the surface at a molecular scale, which in turn is reflected in the contact angle for water droplets.

When the water overlayer has formed (within nanoseconds), natural ions, *e.g.*, Cl^- and Na^+, enter the

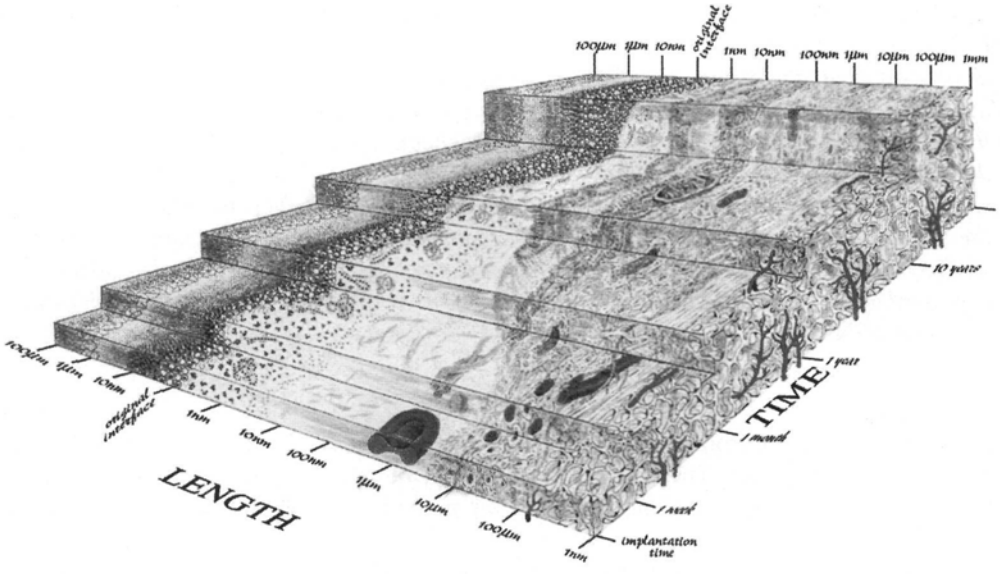

Fig. 1—A "bird's eye" view of the temporal development of the interface between a metal implant and the biological tissue. Initially, the implant surface is exposed to a bioliquid (blood) containing water, solvated ions, and biomolecules. As a result of the surgical procedure, there is a zone of damaged tissue around the implant. With time, the tissue heals and starts to grow toward the implant surface. Also indicated is the in vivo *growth of the surface oxide. In favorable cases, a close integration between the tissue and the implant may result, although there may still be a thin (10 nm) separating organic layer adjacent to the implant surface. The vertical part of each staircase step corresponds to an instantaneous picture of the interface at the time indicated on the time axis. The horizontal part of each step illustrates the development of the interface with time. The sizes of the indicated structures should be seen only as approximate dimensions (adapted from Kasemo and Lausmaa, 1986).*

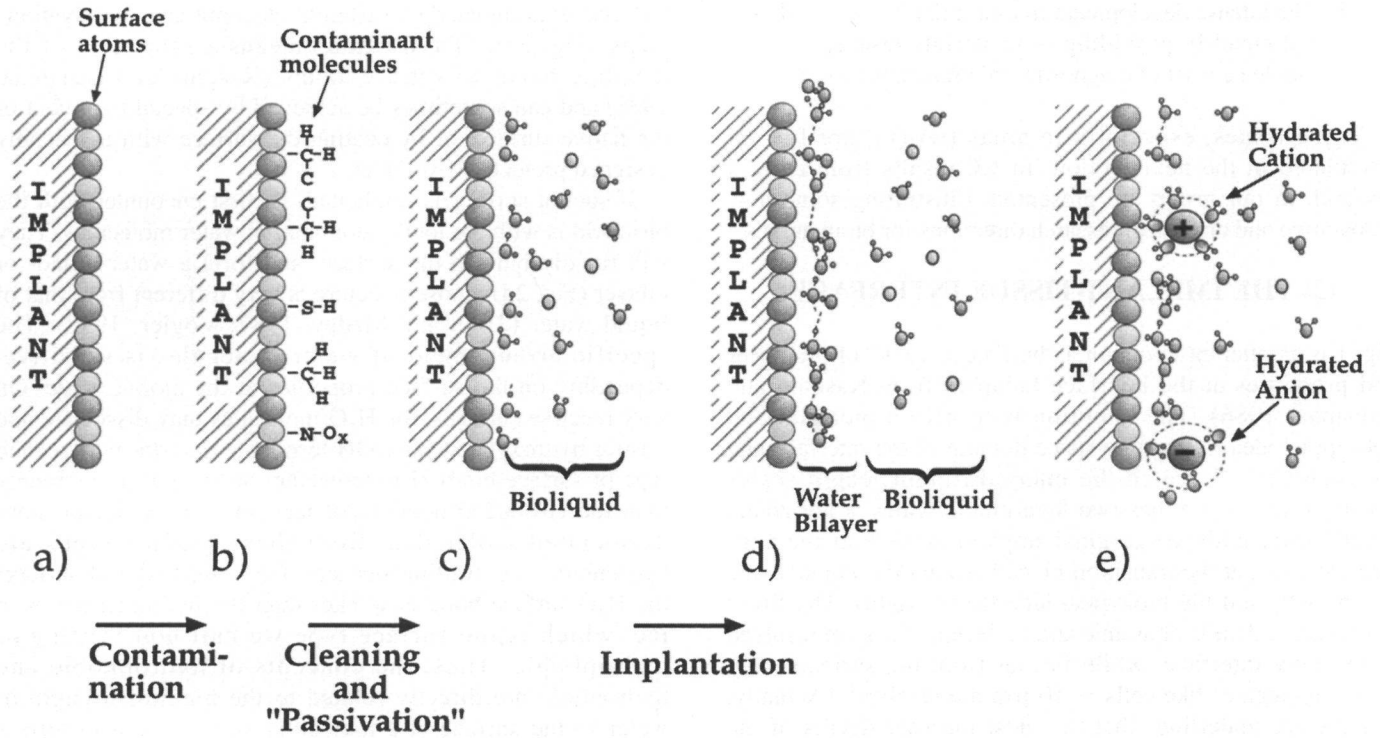

Fig. 2—Schematic illustration of events at the implant surface which occur over time from the initial manufacturing of the implant, to the subsequent implantation of the material, and the later long-term incorporation of the implant into the surrounding tissue. (a) An originally clean surface with the outer atomic layer illustrated. (b) The same surface after exposure to the ambient environment, which contaminates the surface with organic and inorganic compounds. (c) Removal of contamination layers and passivation of the implant surface by saturation of all dangling bonds of the outer atomic layer. (d) Immediately after implantation, water will bind at the surface; in this case, a bilayer of intact water molecules forms at a hydrophilic surface. (e) Hydrated ions, such as Cl^-, Na^+, and Ca^{++}, will be incorporated into the surface water layer, the extent of which depends on the electrostatic double layer at the surface of the implant material. (f) Blood proteins find their way to the surface, and adsorb and desorb according to their relative concentration and size in the surrounding liquid, and electrostatic and hydrophobic interactions with the surface. The proteins may adsorb intact or may denaturate to minimize the free energy of the system. (g) Eventually, more blood proteins and tissue-specific proteins come to the surface, and we obtain a mixture of protein types, possibly in different conformation states. (h) By the time cells arrive at the interface, they see an ionically screened and protein-coated implant surface. The types and conformations of the proteins at the surface will strongly determine which cells bind, how they bind, and if they become activated by adhesion receptors binding to peptide sequences expressed on the adsorbed protein surface. (i) The activity of cells at the interface participates in determining the type of tissue which grows up to the implant surface, e.g., *fibrous capsule* vs. *mature tissue.*

interface and are incorporated into the water overlayer as hydrated ions (Fig. 2e). The specific arrangement of these ions, and their water shells, is influenced by the properties of the surface.

Yet a little later, the biomolecules in the bioliquid surrounding the implant reach the surface (Fig. 2f) and adsorb there in a complex series of events, including initial adsorption, maybe conformational changes/denaturation and/or replacement by the so-called "Vroman effect", when (typically) smaller proteins are eventually replaced by larger proteins. Since there are many different proteins in the bioliquid, the composition of the protein adlayer will be a mixture of the proteins that arrive early and those which arrive later but have stronger binding to the surface (Fig. 2g).

An important fact to underline is that different surfaces provide very different opportunities for protein binding (Lundström, 1985; Horbett and Brash, 1995; Brash and Wojciechowski, 1996; Hlady and Buijs, 1996; Norde, 1996). Thus, both the exact mixture of proteins on the surface and their conformational state(s) will be different, depending on the original surface properties, *e.g.*, how the surface binds water (Israelachvili and Wennerstrom, 1996). The latter lies behind the common observation that, *e.g.*, hydrophilic and hydrophobic surfaces bind proteins differently. On very hydrophilic surfaces, it is more likely that proteins bind with their hydrophilic areas toward the surface, and with intact water shells, while on very hydrophobic surfaces, the proteins are more likely to bind with their hydrophobic segments closest to the surface, and without intervening water shells.

When the protein layer has been established (it is probably never totally static, but rather subject to slow dynamic changes in composition and conformational state, since the

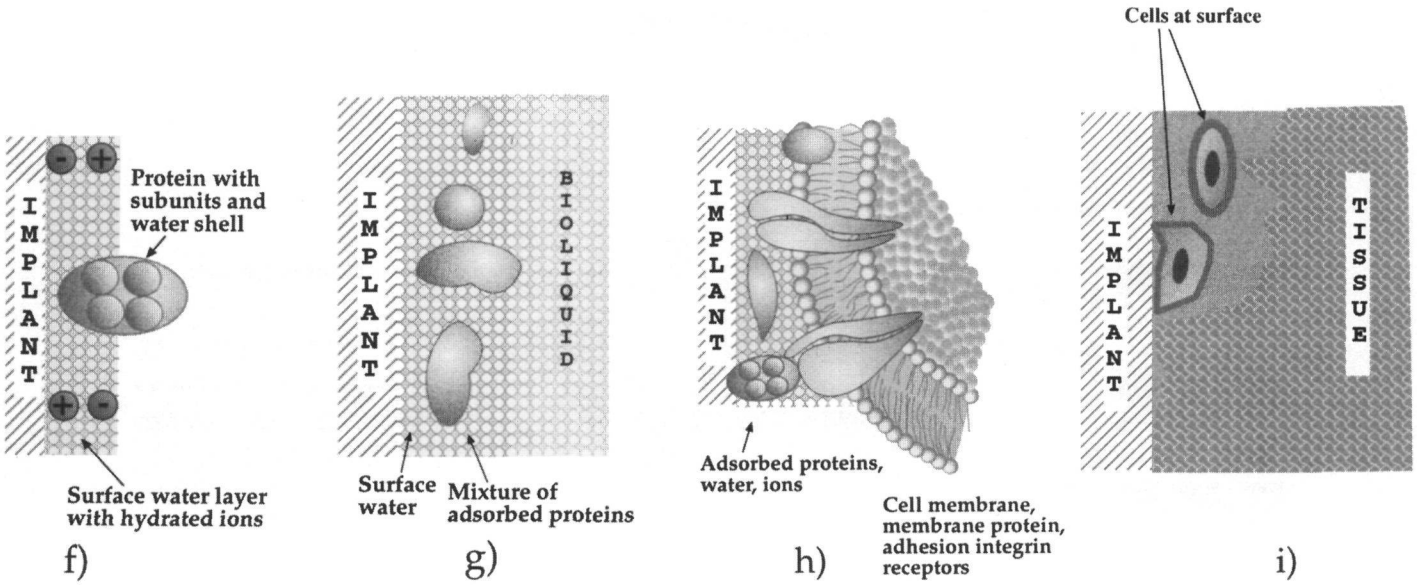

composition of the bioliquid outside the surface changes over the whole healing period), living cells appear on the stage. They are biological aggregates from 100 to 10,000 times larger than the proteins and enormously much more complex in structure and function. They interact with the protein-covered surface *via* the cell extensions reaching the surface, *via* their cell membrane, and *via* membrane-bound proteins and receptors (Fig. 2h). The surface specificity of the cell-surface interaction derives, at least partly, from how the protein layer is composed and organized, which in turn depends on how the surface binds water, ions, and different biomolecules. There is thus no need of a direct cell-surface contact for a surface specific cell interaction to be obtained. The result of such interactions could be the eventual formation of newly organized tissue at the interface *vs.*, *e.g.*, a chronic inflammatory response to the material (Fig. 2i).

A second potentially important mechanism by which the surface may affect the cells, and ultimately the global tissue response, is if the surface releases ions or molecules that can penetrate the cell membrane or activate membrane-bound receptors. Such positive stimuli can be of an inorganic nature, as in the case of Ca^{++} and PO_4^{--} ions from calcium phosphates, or more complex organic molecules, such as growth hormones or enzymes. Negative stimuli can be corrosion products, which can be, *e.g.*, allergenic.

A third important factor, not included in the scenario above, is that both protein-surface and cell-surface interactions are also influenced by the surface microtopography, as illustrated schematically in Fig. 3. Curved surfaces, pits, protrusions, cavities, etc., that have sizes and radii of curvature comparable with those of the biological entities (proteins ~ 1-10 nm, cells 1-100 μm) will induce biological interactions different from those on a flat surface.

The main intention with the scenario of Figs. 1-3 is to argue that there is a causal connection between the detailed properties of a native implant surface and the ultimate tissue response. The relative importance of different surface properties *in vivo* is still largely unknown. If we consider two major classes—namely, the chemical composition and the structural and topographic properties such as curvature, porosity, roughness, etc.—it seems today that the latter have a larger importance than was believed 10-15 years ago. The most correct view on surface chemistry and micro-architecture is to treat them as simultaneously important and synergistically influencing the tissue response. Generally, we thus expect that the biological system recognizes the surface

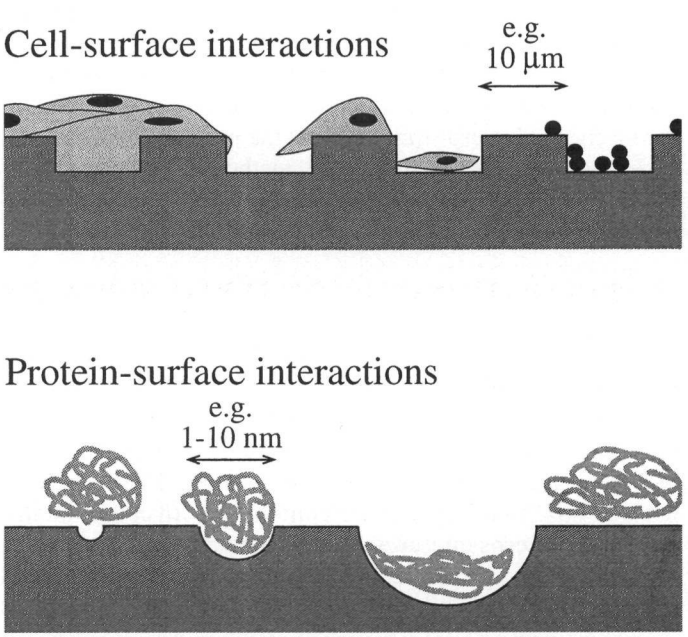

Fig. 3—Topographical features on the implant surface most likely influence biological interactions at the interface. Pits, protrusions, and steps of dimensions similar to those of proteins (ca. ≤ 40 nm) and cells (ca. ≤ 20 μm) can cause a change of the morphology and activity of these bioactive entities as compared with flat surfaces.

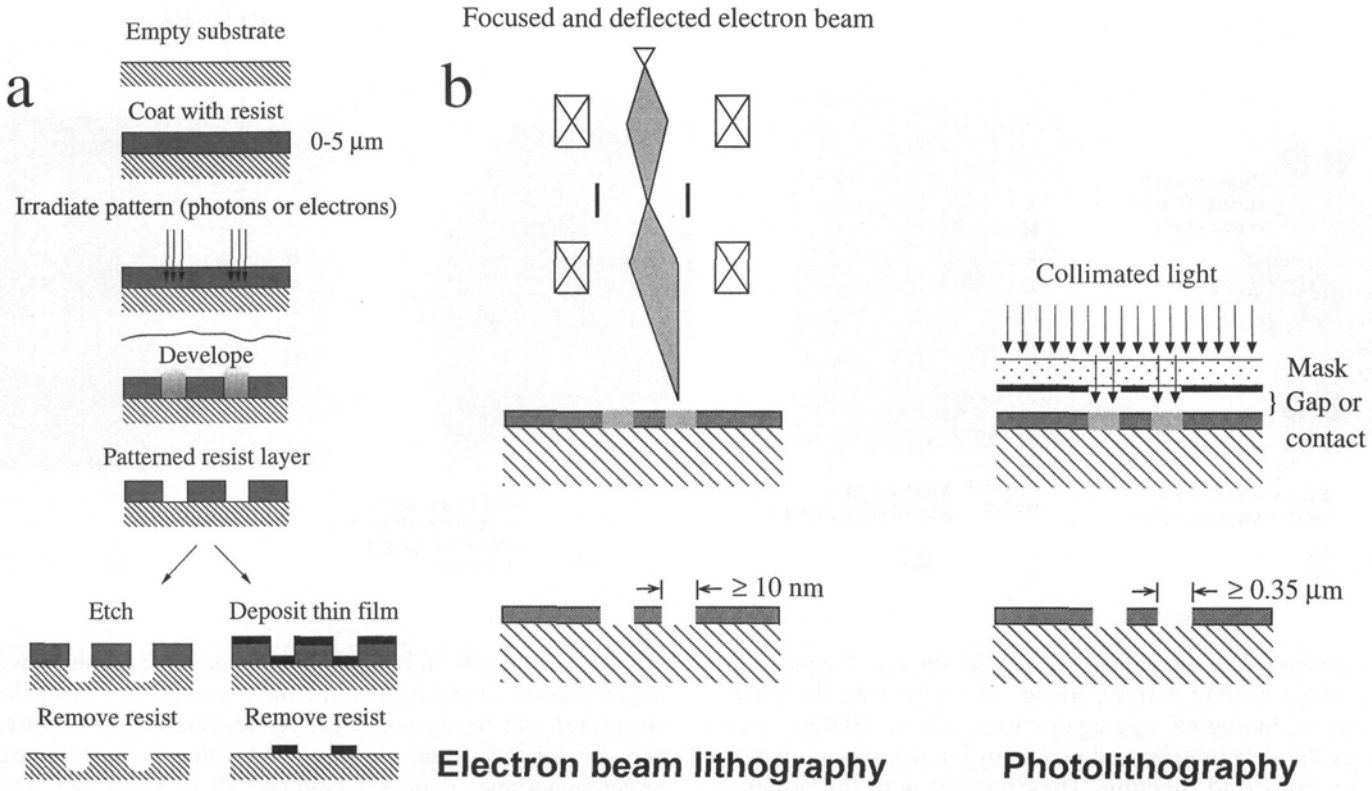

Fig. 4—(a) Basic step-wise production procedure for lithographically fabricated surfaces, where the final steps are typically etching a pattern into the substrate (left) or depositing a patterned thin film onto the surface (right). (b) Comparison of electron beam lithography (left) and photolithography (right) in terms of throughput of each method and feature sizes obtainable.

through the combined topographic and chemical pattern that the surface exposes (Ratner, 1996). The third factor—adding to these two—is the micromechanical or viscoelastic properties of the surface, which can affect (enforce or reduce) the mechanical stress-strain fields at the interface.

In the remainder of this paper, methods of preparation of biomaterial surfaces, as well as *in vitro* evaluation, are exemplified by recent research results from our group.

(3) PREPARATION OF BIOMATERIAL SURFACES

Today, there exists a large number of preparative tools for tailoring a biomaterial surface. They involve controlled cleaning and oxidation by glow discharge plasma techniques, thin film growth, and deposition of organic overlayers such as polymers, amino acids, peptides, and proteins. These chemical surface modifications can be combined with intentionally produced microstructures, aimed at matching biological components or inducing desired biological reactions. The size ranges of interest include the smallest proteins (~ 1 nm) and the largest cells (< 100 µm). Most common early methods to produce 3-D topographic patterns of surfaces involved sandblasting and other mechanical methods, wet chemical etching, and plasma spraying (Thomas and Cook, 1985; Inoue *et al.*, 1987; Wilke *et al.*, 1990). More recently, much more refined lithographic techniques (Hirono *et al.*, 1988; Chehroudi *et al.*, 1990; Singhvi *et al.*, 1994; Meyle *et al.*, 1995; Nakayama and Matsuda, 1995) and techniques based on, *e.g.*, sol systems have been used (Douglas *et al.*, 1986; Pum *et al.*, 1991; Hulteen and vanDuyne, 1995; Hanarp *et al.*, 1999).

(3.1) Lithographic patterning of surfaces

The basic principle of the lithographic techniques (Fig. 4a) is, first, to cover the surface with a radiation-sensitive film—usually a polymer called 'resist'—then expose certain areas of the film to a beam of radiation which modifies the polymer properties at the irradiated areas. The latter can then be removed by dissolution, leaving a pattern of polymer on the surface that serves as a mask for surface treatment of the uncoated areas. The exact pattern on the surface is produced, for example, by illuminating the polymer film through a pre-designed mask (in the case of photolithography; Fig. 4b, right) or by steering the radiation beam to desired positions (as in electron beam lithography; Fig. 4b, left). The surface treatment of the areas where the polymer was removed can be simple etching (to create pits, grooves, etc., of controlled shape and size; Fig. 4a, lower left) or deposition of overlayers (Fig. 4a, lower right) by, *e.g.*, evaporation or self-assembled monolayers. The smallest feature size obtainable by conventional photolithography is around 0.3 µm, while electron beam lithography can produce features down to below 10 nm, depending on processing procedures and materials being patterned.

Some examples of surfaces produced by lithographic

patterning at different size scales are shown in Figs. 5 and 6. Larger features, on the order of microns, are produced by photolithography (Fig. 5). Since many features can be patterned at once, this method is quick and is currently used by the microelectronics industry for large-scale production of integrated circuits. Fig. 5 shows a micropatterned surface of polymethylmethacrylate (PMMA). The 5-μm cubes were created by ion-beam-etching the PMMA surface after it was masked by a patterned polymer film. In this case, the pattern was a matrix of 5-μm squares. It is possible to vary the cube dimensions and spacings by changing the pattern definition (*i.e.*, the mask) and etching time.

When features of smaller dimensions are being patterned, such as nanometers, radiation sources with wavelengths similar to those of the desired feature sizes must be used. For example, we have used electron beam lithography to pattern surfaces with sub-micron features (Gold *et al.*, 1995; Wong *et al.*, 1996; Kasemo and Gold, 1997; Hedberg *et al.*, 1999). An example of 20-nm-wide pits, produced by electron beam lithography and ion beam etching, is shown in Fig. 6. Features on this size scale can influence the adsorption of proteins at the surface, for both topographical as well as chemical reasons, since the material in the bottom of the pits in this case is NiCr and has chemical properties different from those of the surrounding Au surface.

One drawback of electron beam lithography is that it is slow (to pattern a 1-cm^2 area with features of these dimensions would take hundreds of hours; additionally, features are "drawn" on the surface one at a time) and very difficult to execute on non-planar surfaces, due to focusing problems. However, due to the need for increased miniaturization in microelectronics, the technology development is very fast in this area, and faster equipment is already appearing on the market.

(3.2) Laser patterning

An entirely different method for making surface patterns is based on the possibility of focusing an intense laser beam at certain spots on a surface, where the high beam intensity causes evaporation of the material. By this approach, pits can be produced down to ~ 1 μm, *i.e.*, in the size range of interest to match cell sizes. By controlled motion of the beam (either by using clever optics or by sample motion), pre-designed patterns can be made.

It is impractical to pattern a surface, *e.g.*, an entire dental implant, by ablating one pit at a time. This problem can be circumvented by the use of a kinoform. A kinoform is a diffractive optical element (a computer-generated micro-optic component that uses diffraction to manipulate light) which diffracts a laser beam into multiple beams at controlled, predetermined positions (Lesem *et al.*, 1969; Ekberg *et al.*, 1991; Larson *et al.*, 1994). It can be used to create multiple, parallel beams with equal intensity in each beam. With a kinoform, it is possible to "laser-machine" mutliple pits in a surface at once (Ekberg *et al.*, 1991), an example of which is shown in Fig. 7 (top) (Jartoft and Krantz, 1997). The kinoform pattern can be positioned and focused at different locations on complex surfaces, such as the flanks of a titanium dental implant (shown in the bottom of Fig. 7) (Jartoft and Krantz, 1997). The shapes of the pits can, in principle, be chosen arbitrarily. As for photolithography, the allowable sample surface height deviation is determined by the depth of focus of the lens in the optical set-up.

(3.3) Colloidal-based fabrication techniques

One method for increasing the speed of patterning surfaces with nano-sized features is to use colloidal particles as lithographic masks. Colloidal particles of different materials can be produced with monodisperse size distributions down to nm sizes. By control of the properties of the solution in which the

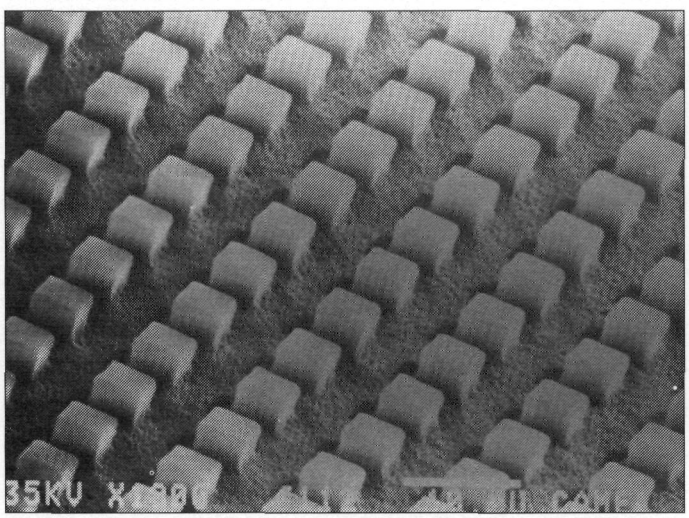

Fig. 5—Cubic structures (ca. 5 μm) protruding from the surface of a piece of polymethylmethacrylate (PMMA), produced by photolithography and chemically assisted ion beam etching in Ar and O_2 gases. Such surface features are expected to affect cell adhesion and function at the interface. Scale bar = 10 μm.

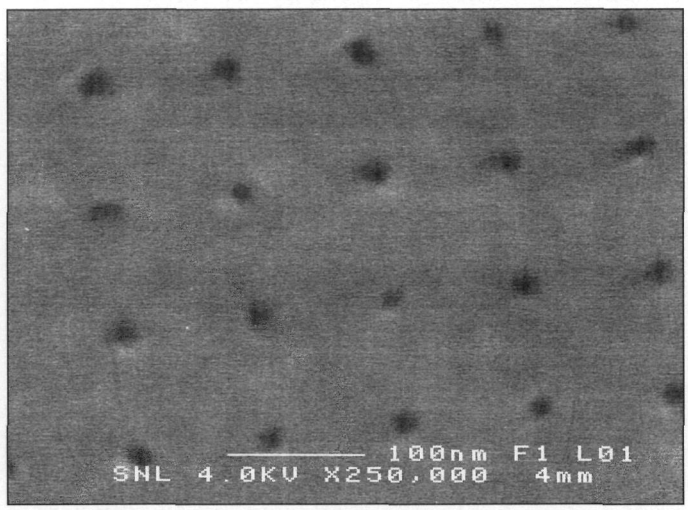

Fig. 6—Thin gold film with nanopits (20-nm diameter, 100-nm spacing) produced by electron beam lithography and Ar^+ ion etching. The pits are approximately 15 nm deep and contain NiCr at the bottom. Features on this size scale can influence adsorbed protein location, conformation, and activity; however, the production method is slow. (Photograph courtesy of D. Sutherland)

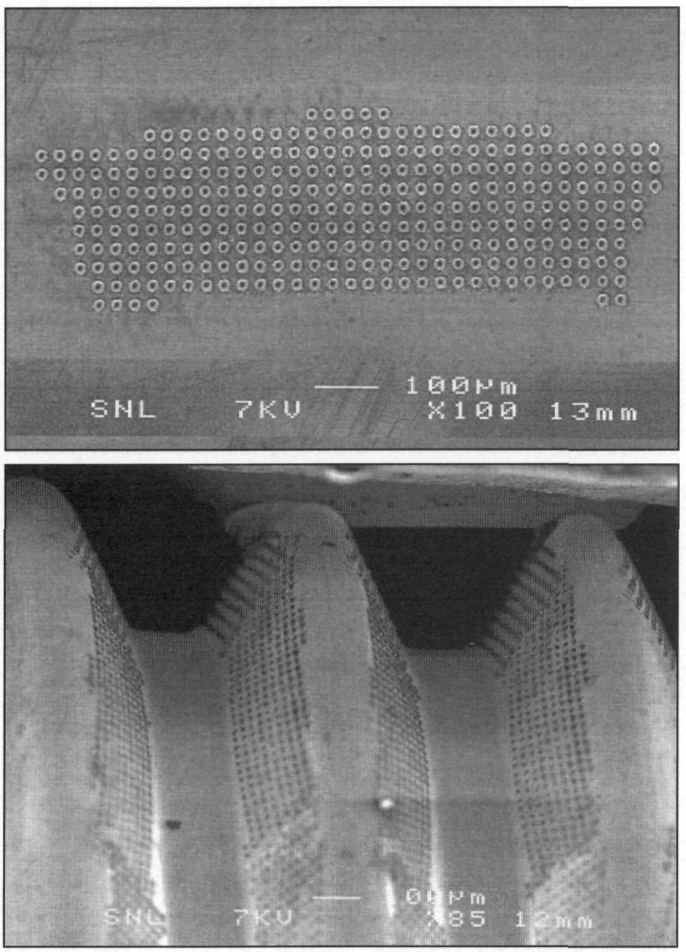

Fig. 7—Laser micromachining is an easier method to vary the spacing, sizes, and patterns of features produced on a surface compared with traditional lithographic methods. By the use of a kinoform (i.e., *a diffractive optic element), it is possible to laser-machine many pits simultaneously (top image) and thereby increase the speed of the micropatterning method. The kinoform splits the laser beam into multiple beams with equal intensity in all spots. Pits (from 10 to 20 µm in diameter) were laser-machined on the thread flanks of a titanium screw-shaped dental implant (lower image). (From Jartoft and Krantz, 1997)*

colloidal particles are kept, it is possible to control how such particles attach to a surface (Johnson and Lenhoff, 1996; Persson *et al.*, 1998; Hanarp *et al.*, 1999). It is possible, for example, to deposit monolayers of uniformly distributed particles (Krozer *et al.*, 1995). The particle density in the monolayer can be controlled by the salinity (Hanarp *et al.*, 1999) (Fig. 8) and pH of the solution. Also, multilayers of particles can be deposited (Krozer *et al.*, 1995), thus constituting a porous surface where pore size is scaling with the particle size. Such mono- or multilayers of deposited particles (*e.g.*, metal oxide particles like SiO_2, TiO_2, polymer particles, etc.) are of interest themselves as biomaterial surfaces through the topographic patterns and the porosities they represent (Hanarp *et al.*, 1999).

Adsorbed colloidal particles can also be used as templates or masks for patterning of the underlying surface, schematically illustrated in Fig. 9a. The colloidal particles can serve as etch masks of the underlying substrate (Fig. 9a, left) and also as lift-off masks (Fig. 9a, right). In the first case, the substrate surrounding the particles is etched, leaving the areas under the particles as protrusions. In the latter case, the surface surrounding the particles is built up by the deposition of a thin film onto the particle-covered surface. The particles are then removed, and the orginal underlying surface is exposed in the location of the particles. With both methods, it is possible to achieve simultaneous nanoarchitecture and spatially patterned surface chemical properties.

An example of a colloidal lithographically patterned substrate is shown in Fig. 9b. It was prepared by means of 110-nm polystyrene (Latex) particles bound to a gold surface (unpublished observations). An 8-nm-thick titanium oxide layer was deposited, and the particles were removed by a tape-striping method. This left 100-nm-diameter pits through the oxidized titanium layer, with gold exposed at the bottoms of the pits.

One of the main benefits of using colloidal lithography compared with the other lithographic methods is that complex sample shapes with non-planar surfaces can potentially be patterned with nanometer-sized features or coated with nanoporous layers.

(4) *IN VITRO* EVALUATION OF BIOMATERIAL SURFACE PREPARATION AND PERFORMANCE BY THE QCM-D TECHNIQUE

There is an urgent need for techniques that can follow depositions on biomaterial surfaces such as those illustrated in Figs. 2f-2h *in vitro* and in real time. One such area of interest is measurement of the dissolution or precipitation rates of inorganic surface deposits such as calcium phosphates. Maybe even more interesting is the measurement of the adsorption kinetics of polymers, peptides, proteins, and biomembranes, and the adhesion dynamics of living cells. Several techniques have been applied successfully to some of these deposition types (Lundström, 1985; Horbett and Brash, 1995; Brash and Wojciechowski, 1996; Hlady and Buijs, 1996; Norde, 1996), *e.g.*, ellipsometry (Arwin, 1998; Elwing, 1998; Tengvall *et al.*, 1998), surface plasmon resonance (Kösslinger *et al.*, 1995), and total internal reflection spectroscopy (Axelrod *et al.*, 1984; Hlady *et al.*, 1990).

In the present section, we describe results obtained with a technique called the dissipative quartz crystal microbalance, QCM-D (Rodahl *et al.*, 1995). The conventional quartz crystal microbalance (QCM) is based on measurement of the frequency shifts of a piezoelectric sensor, oscillating in the shear mode due to an externally applied electric field. The sensor is typically disc-shaped, from 10 to 25 mm in diameter, and ~ 0.1 to 0.3 mm thick. The sensor crystal is placed in a measurement cell so that (typically) one of the sensor sides is facing the liquid.

The excited (driven) crystal performs a shear oscillatory motion with a constant frequency (typically 5 to 10 MHz) and constant amplitude (< 1 nm), as long as the environment does not change. The oscillatory motion is damped due to (i)

inherent energy losses in the crystal, (ii) energy losses due to any overlayer deposited on the sensor, and (iii) energy losses to the surrounding medium. One can measure the magnitude of the sum of these losses (Rodahl *et al.*, 1995) by suddenly switching off the driving field to the sensor crystal, whose oscillation then rapidly decays in amplitude. This decay has the form of a damped sinusoidal wave, characterized by the frequency, f, of the sensor crystal+overlayer+surrounding liquid, and by the time constant, τ, for the damping. The latter is inversely proportional to the sum of the dissipative mechanisms mentioned above and is called the dissipation factor, D. The QCM-D technique is based on simultaneous measurements of f and D.

If there is a change in the conditions of the sensor crystal, *e.g.*, deposition of a cell or protein overlayer on its surface, both the frequency and the dissipation factor will change by magnitudes Δf and ΔD, which are related to the deposited mass (by proportionality if certain conditions are fulfilled) and to the viscoelastic and dissipative properties of the overlayer. Thus, by continuous measurement of Δf and ΔD during, *e.g.*, a protein or cell deposition experiment, information is obtained both about the deposition kinetics and the amount of deposited biological matter (through Δf), and about the viscoelastic properties of the overlayer (through ΔD). The measurement is performed with real-time recording at ~ 1 Hz, with a resolution in f corresponding to fractions of a monolayer of proteins, and with resolution in D sufficient for detection of dissipative losses in fractions of protein monolayers. Practically, the measurement consists of injecting or "flowing" the desired solutions into a small measurement cell, where the sensor crystal is placed. The particular material to be studied is deposited as a thin film onto the surface of the sensor. The thickness of the film lies in the range 1 nm to 1 μm, depending on the type of material and the experiment.

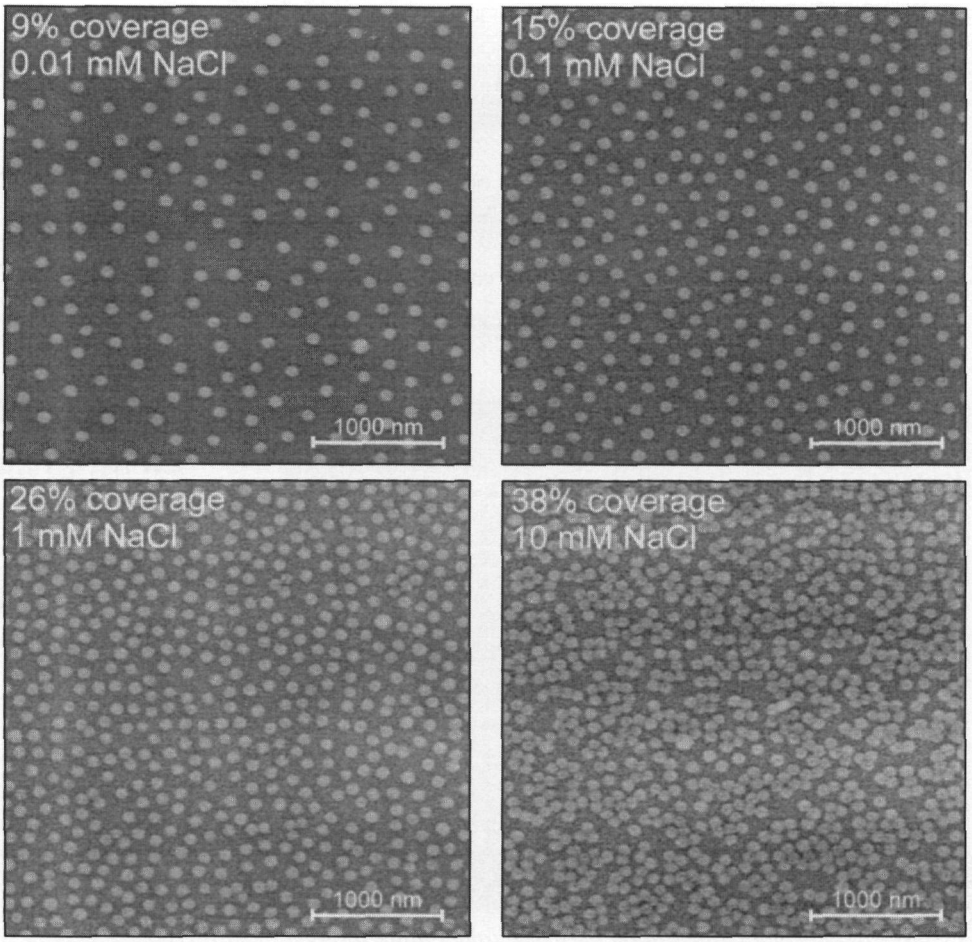

Fig. 8—Colloidal polystyrene Latex particles (110 nm, negatively charged), deposited onto titanium surfaces from solutions having different salt concentrations (as indicated), form sub-monolayers of quite uniform nearest-neighbor spacing at low % coverage. (From Hanarp et al.*, 1999)*

(4.1) Protein adsorption

The QCM-D method has been used to study adsorption kinetics of a large number of proteins (Höök *et al.*, 1997, 1998a,b; Rodahl *et al.*, 1997), *e.g.*, myoglobin (Mb), albumin (HSA), hemoglobin (Hb), ferritin (Fer), and fibrinogen on different surfaces; adsorption/deposition of vesicles and lipid monolayers (Keller and Kasemo, 1998); and cell deposition on different surfaces (Fredriksson *et al.*, 1998; Nimeri *et al.*, 1998). Three examples are shown in Figs. 10-12. Figs. 10a and 10b show the deposition of HSA, Hb, and Fer as frequency (mass) change *vs.* time (Fig. 10a) and dissipation change *vs.* time (Fig. 10b). The surface was a hydrophobic surface consisting of a monolayer of methyl-terminated thiol molecules on gold. Qualitatively, Fig. 10a reflects how the proteins initially adsorb very rapidly, and then the deposition slows toward a saturation value. Quantitative analysis shows that the saturation amounts correspond to, respectively, a nearly close-packed monolayer for HSA, a bilayer for Hb, and a monolayer for Fer. The bilayer interpretation for Hb is partially based on the magnitude of the Δf value at saturation, and partially on the shape of the ΔD *vs.* Δf curve (not shown). As discussed in Höök *et al.* (1998a), the latter is consistent with an early deposition of (partially) denatured Hb in the first monolayer, and subsequent adsorption in a second layer of intact, native Hb molecules.

(4.2) Biomembrane adsorption

Figs. 11a and 11b show the Δf (t) and ΔD (t) traces, respectively, recorded when a hydrophilic silicon oxide surface was exposed to sonicated phosphatidylcholine vesicles of radii ~ 12.5 nm. Very interesting ΔD (t) and Δf (t) behavior is

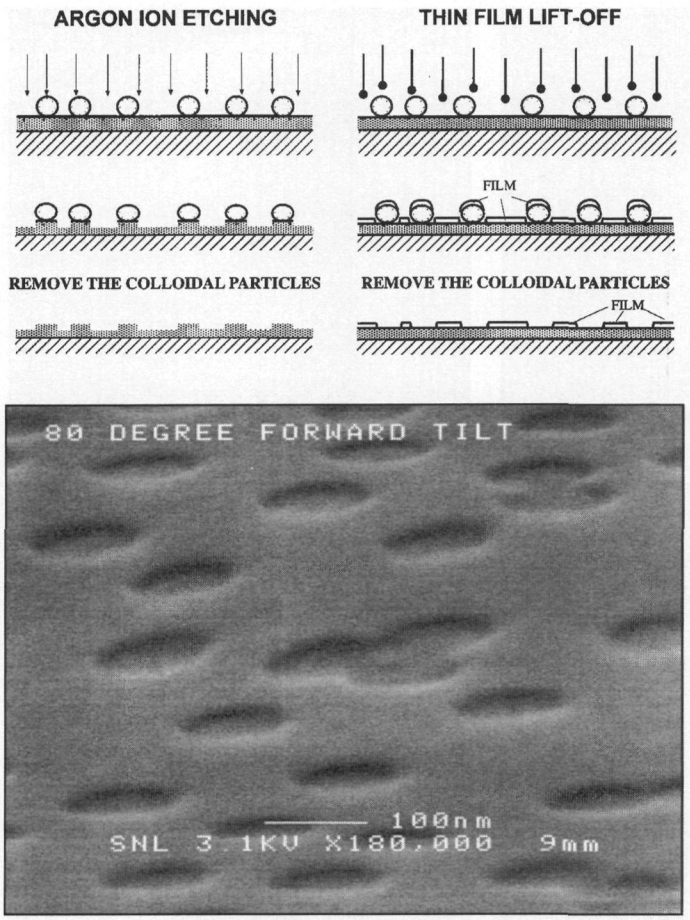

Fig. 9—(a) Schematic illustration of two colloidal lithography methods for patterning substrates. Particles can be used as etch masks for removing material from the underlying surface (left), or as lift-off masks during thin film deposition (right). (b) SEM micrograph of 110-nm-diameter pits produced in titanium oxide by colloidal lift-off lithography. The pits are 8 nm deep and contain gold at the bottom. (Images courtesy of D. Sutherland)

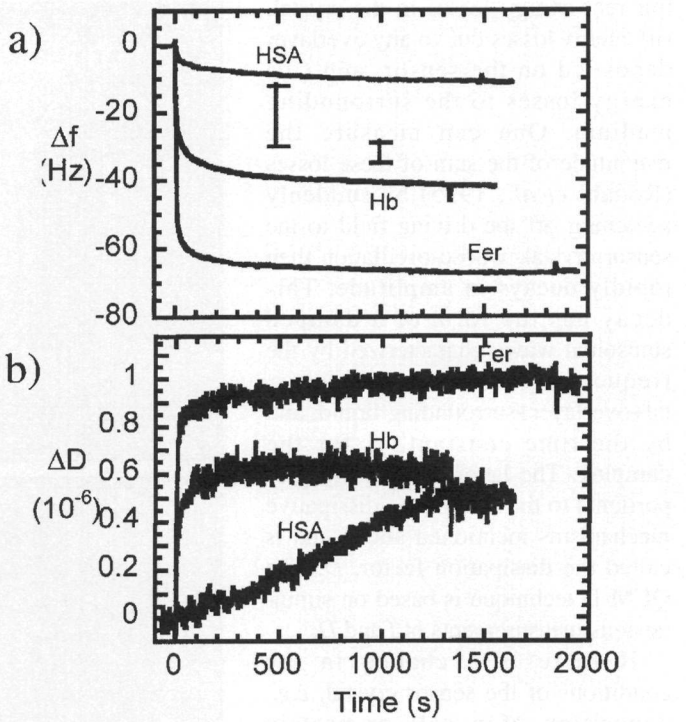

Fig. 10—The quartz crystal microbalance (QCM-D) frequency shift (a) and dissipation shift (b) vs. time for HSA, Hb (pH 7.0), and Fer adsorption on gold, covered by a hydrophobic methyl-terminated thiol monolayer. The proteins were introduced at t = 0. The vertical bars in (a) represent the range of frequency shifts expected for monolayer coverage of the respective proteins (depending on protein configuration at the surface). (From Höök et al., *1997)*

observed: Initially, a large decrease in frequency (increase in mass) and increase in dissipative losses are observed, followed by rapid reversal of the signals toward less mass and less dissipation. Following is the interpretation arrived at (Keller and Kasemo, 1998) when these results were compared with corresponding results for a hydrophobic surface and another even more hydrophilic surface compared with that from which Fig. 11 is obtained:

Initially, intact vesicles are adsorbed. Due to their large mass and flexibility, they yield large f and D shifts. Suddenly, the vesicles break and deposit a lipid bilayer (thereby causing a mass loss through the loss of water trapped inside the vesicles), and finally forming a continuous lipid membrane on the surface. The latter is more rigid than the intact vesicles and therefore causes less dissipation—that is, a smaller D-shift. This explains the minimum in Δf (t) and the maximum in ΔD (t).

A convenient and illustrative way to display the complex dynamics of membrane deposition on a surface is to plot ΔD *vs.* Δf, thus eliminating time as an explicit parameter (Fig. 11c). Such *D-f* plots clearly reveal two different kinetic phases: the initial intact vesicle adsorption, and the later lipid bilayer formation.

(4.3) Cell adhesion

The last example concerns characterization of cell adhesion to different surfaces. Several recent studies (Fredriksson *et al.*, 1998; Nimeri *et al.*, 1998) have shown that the QCM-D measurements provide a very fast and informative way of measuring some aspects of cell-surface interactions in real time. We have chosen to discuss measurements of the interaction of human neutrophils with protein-coated surfaces (Nimeri *et al.*, 1998). This topic is of particular interest to the fields of dental and medical implants, since neutrophil activation is one of the first events in the response to foreign material in the body. Fig. 12 shows the evolution of the ΔD (t), Δf (t), and ΔD *vs.* Δf signals after deposition of approximately 2000 neutrophils on an uncoated polystyrene surface, while Fig. 13 shows the response for a comparable cell deposition on an IgG-coated polystyrene surface. The initial increase in D and the concomitant decrease in f (phase I) reflect the progressive attachment and spreading of the cells. Both surfaces are known to induce cell spreading. The large

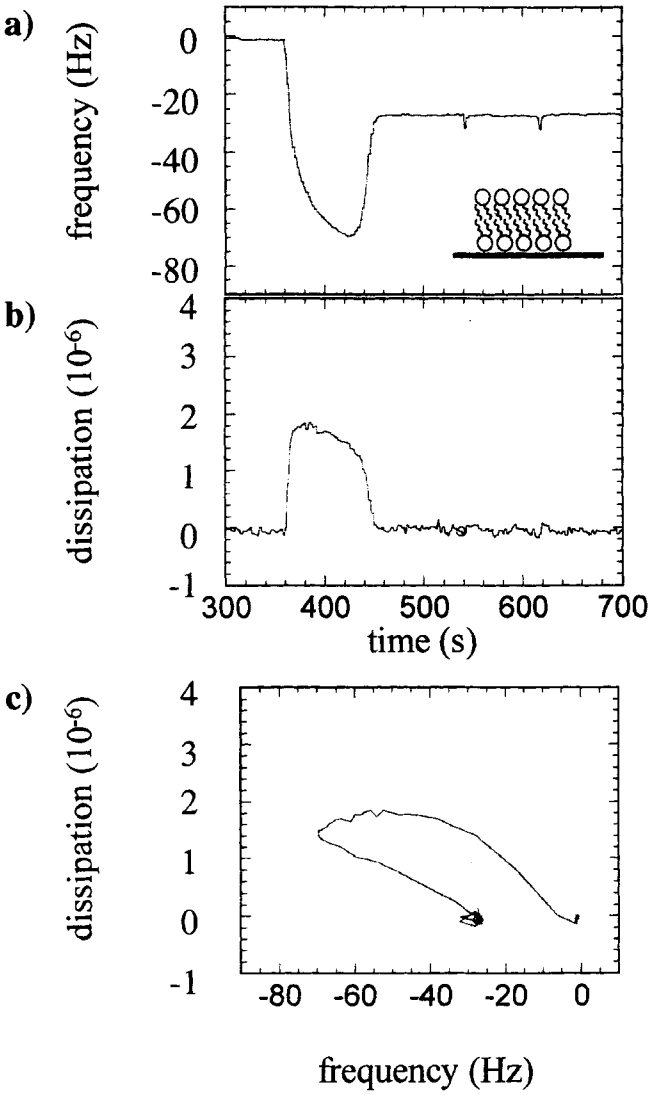

Fig. 11—QCM-D measurements following the adsorption of lipid vesicles to a hydrophilic silicon oxide surface. (a) Frequency shift and (b) dissipation shift vs. *time. (c) The* D-f *plot generated from the data in (a) and (b). By plotting the dissipation shift* vs. *the frequency shift at each time point, one can map the presence of different phases and obtain a "fingerprint" of the adsorption behavior of each adsorbate-substrate system. (From Keller and Kasemo, 1998)*

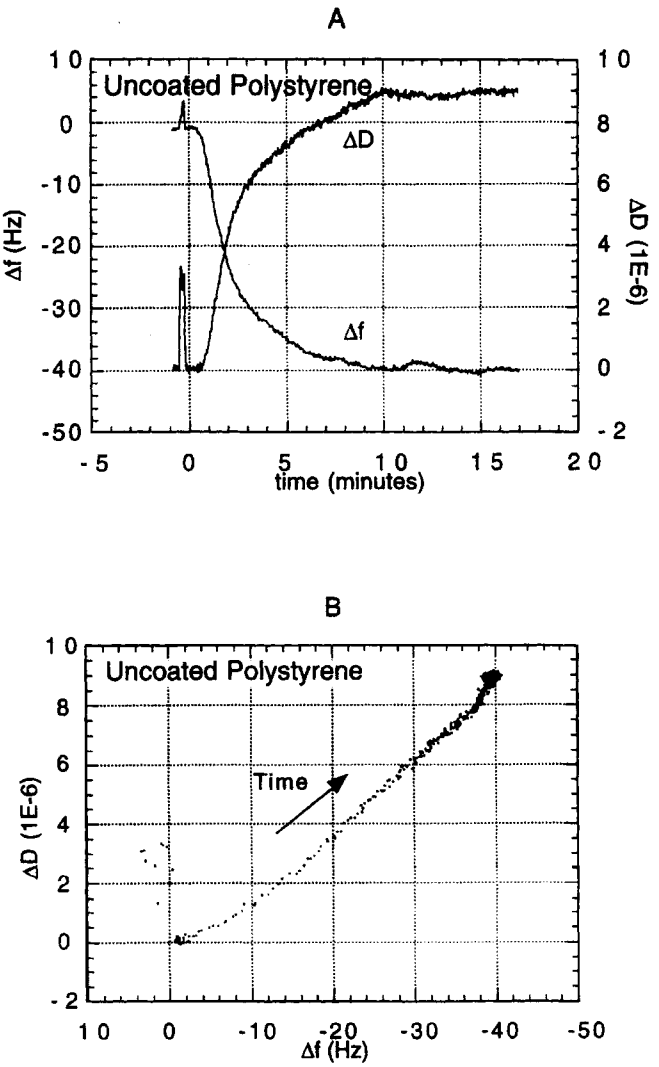

Fig. 12—The QCM-D response for approximately 2000 neutrophils deposited on uncoated polystyrene (a) and the characteristic Df-*plot (*ΔD vs. Δf*) based on the same data (b). (from Nimeri* et al., *1998)*

difference between the two surfaces in the magnitude of the initial increase in D shows that the internal structure of the neutrophils, which have receptors for IgG, are affected by the protein coating. The second, reversed phase (II) of the signals for the protein-coated surface probably involves desorption of IgG caused by the secretion of oxidative metabolites and enzymes. The deposition of neutrophils on human serum-albumin- or fibrinogen-coated surfaces (not shown) results in a considerably lower degree of attachment, spreading, and surface degradation. These proteins are also known not to activate neutrophils (Munro *et al.*, 1983; Yan *et al.*, 1995).

Based on these brief examples, and others not shown, it appears that the QCM-D is a useful method both for evaluating preparation procedures of biomaterial surfaces *in vitro*, and for screening of biomaterials with respect to their affinities and adsorption kinetics for different proteins and living cells. For the latter application, it should be pointed out that the method is fully compatible with simultaneous optical microscopy, fluorescence microscopy, bioluminescence detection, and several other analytical methods.

(5) FUTURE DEVELOPMENTS

Future developments of biomaterial surfaces will include more and more sophisticated and multi-(bio)functional surfaces (Ratner, 1996; Sackmann, 1996). The latter include the following aspects, partly illustrated by Fig. 14:

(i) An almost revolutionary development is ongoing with

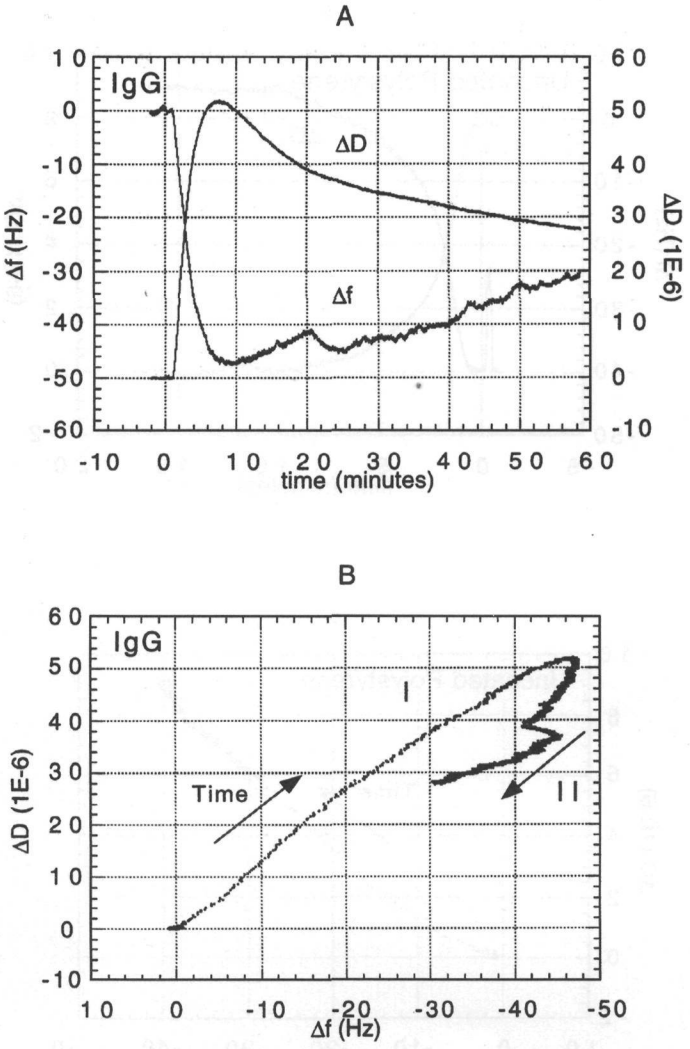

Fig. 13—The QCM-D response for approximately 2000 neutrophils deposited on IgG-coated polystyrene (a) and the characteristic Df-*plot (*ΔD vs. Δf*) based on the same data (b). The evolution with time and the two phases of the signal (I and II) are indicated in the* Df-*plot. (From Nimeri* et al.*, 1998)*

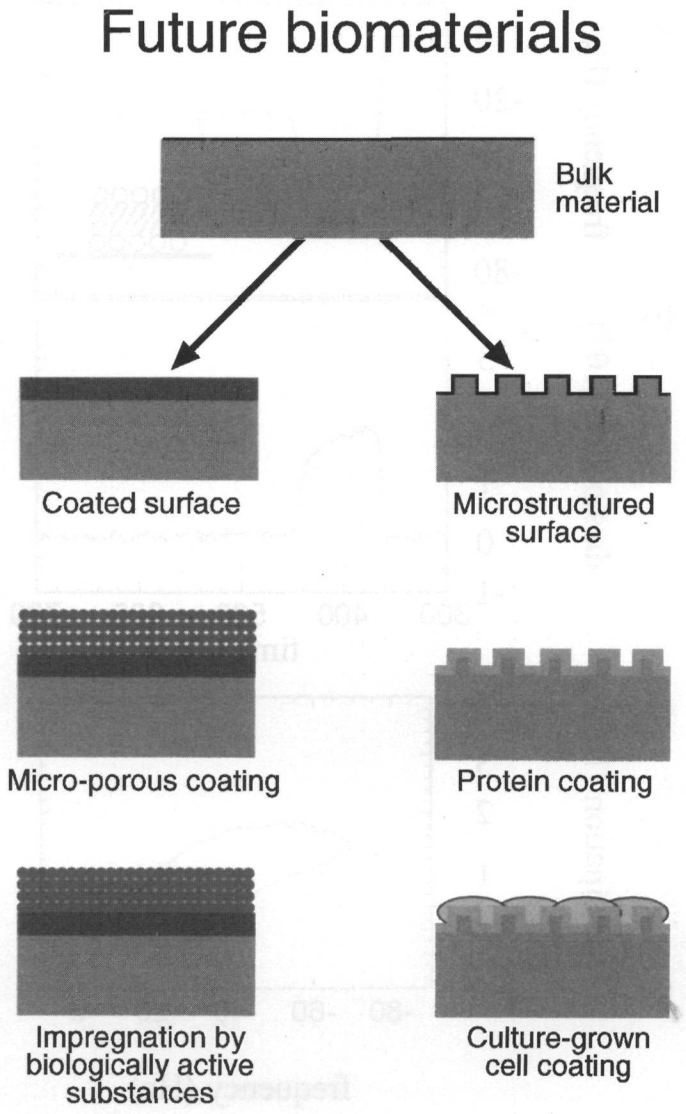

Fig. 14—Surface modification will play a major role in the generation of future medical implant materials. Some ideas are schematically illustrated, where biologically active as well as time and functionally programmed surfaces will meet the needs of cells and tissues at the interface at different times during the healing process.

regard to the possibilities for building up the micro-architecture of surfaces. This will be exploited to optimize the 3-D surface architecture, with the intention of functionally matching different biological entities such as proteins, cell processes, and whole cells. This matching aims at recognition at both the molecular and cell size levels.

(ii) The micro-architectural functionality mentioned under (i) will be combined with corresponding chemical patterns working in synergy with the micro-architecture.

(iii) Controlled surface porosity will provide new functions, influencing cell-surface interaction, transport of nutrients, and signal substances, release of functional additives, etc.

(iv) Programmed dissolution of multilayered surfaces provides new opportunities to optimize the biomaterial surface for different periods of the healing-in phase. Such time programming of the surface can be used to expose different micro-architectures, different chemical patterns, and different porosities at different times. It also provides the opportunity of time-programmed release of different inorganic and organic stimuli, like growth hormones.

(v) By the use of soft, viscoelastic overlayers, the mechanical properties of surfaces at the macro- and microscale can be optimized for the interface. Such overlayers may involve, *e.g.*, biomembranes and hydrogels.

(6) SUMMARY AND CONCLUSIONS

We have discussed some trends in biomaterials research over the past 15 to 20 years, focusing on the biomaterial-tissue

interface and especially on surface preparation, characterization, and evaluation of biomaterials. Major progress has been made in problem formulations, working hypotheses, preparation and characterization methods, and *in vitro* evaluation methods. Yet there is a long way to go before we achieve a thorough understanding about the detailed mechanisms and processes determining the temporal and spatial evolution of the biomaterial-tissue interface.

ACKNOWLEDGMENTS

We thank Claes Fredriksson, Fredrik Höök, Craig Keller, Kate Larsson, and Duncan Sutherland for their assistance in the preparation of this manuscript. Most of this work has been performed under the Swedish Biomaterials Consortium, which has been funded for the past 8 years by the Swedish National Board for Industrial and Technical Development (NUTEK) and the Swedish Natural Science Research Institute (NFR), and more recently by the Swedish Foundation for Strategic Research (SSF). Part of this work has been supported by SSF's Biocompatible Materials Research Program, an EU Training and Mobility of Researchers (TMR) Grant, and by Nobel Biocare AB, Göteborg, Sweden. We are grateful to the Swedish Nanometer Laboratory at Chalmers University of Technology, Sweden, where most of the surface modification was performed.

REFERENCES

Albrektsson T, Brånemark P-I, Hansson H-A, Kasemo B, Larsson K, Lundström I, *et al.* (1983). The interface zone of inorganic implants in vivo; titanium implants in bone. *Ann Biomed Eng* 11:1-27.

Arwin H (1998). Spectroscopic ellipsometry and biology: recent developments and challenges. *Thin Solid Films* 313:764-774.

Axelrod D, Burghardt TP, Thompson NL (1984). Total internal reflection fluorescence. *Ann Rev Biophys Bioeng* 13:247-268.

Brash JL, Wojciechowski PB (1996). Interfacial phenomena and bioproducts: bioprocess technology. McGregor WC, editor. New York: Marcel Dekker.

Chehroudi B, Gould TRL, Brunette DM (1990). Titanium-coated micromachined grooves of different dimensions affect epithelial and connective-tissue cells differently in vivo. *J Biomed Mater Res* 24:1203-1219.

Douglas K, Clark NA, Rothschild KJ (1986). Nanometer molecular lithography. *Appl Phys Lett* 48:676-678.

Ekberg M, Larsson M, Bolle A, Hård S (1991). Nd:YAG laser machining with multilevel resist kinoforms. *Appl Optics* 30:3604-3606.

Elwing H (1998). Protein adsorption and ellipsometry in biomaterial research. *Biomaterials* 19:397-406.

Fredriksson C, Kihlman S, Rodahl M, Kasemo B (1998). The piezoelectric quartz crystal mass and dissipation sensor: a means of studying cell adhesion. *Langmuir* 14:248-251.

Gold J, Nilsson B, Kasemo B (1995). Microfabricated metal and oxide fibers for biological applications. *J Vac Sci Technol A* 13:2638-2644.

Hanarp P, Sutherland D, Gold J, Kasemo B (1999). Nanostructured model biomaterial surfaces prepared by colloidal lithography. *Nanostructured Mater* (in press).

Hedberg L, Petronis S, Kasemo B, Xu H, Bjerneld J, Käll M (1999). Nanofabricated substrates optimized for surface enhanced raman scattering. *Nanostructured Mater* (in press).

Hirono T, Torimitsu K, Kawana A, Fukuda J (1988). Recognition of artificial microstructures by sensory nerve fibers in culture. *Brain Res* 446:189-194.

Hlady V, Buijs J (1996). Protein adsorption on solid surfaces. *Curr Opin Biotechnol* 7:72-77.

Hlady V, Lin JN, Andrade JD (1990). Spatially resolved detection of antibody-antigen reaction on solid/liquid interface using total internal reflection excited antigen fluorescence and charge-coupled device detection. *Biosens Bioelectron* 5(4):291-301.

Horbett TA, Brash JL, editors (1995). Proteins at interfaces II. Vol. 602. ACS Symposium Series. Washington, DC: ACS.

Hulteen JC, vanDuyne RP (1995). Nanosphere lithography: a materials general fabrication process for periodic particle array surfaces. *J Vac Sci Technol A* 13(3):1553-1558.

Höök F, Rodahl M, Brzezinski P, Kasemo B (1997). Energy dissipation kinetics for protein and antibody-antigen adsorption under shear oscillation on a quartz crystal microbalance. *Langmuir* 14:729-734.

Höök F, Rodahl M, Kasemo B, Brzezinski P (1998a). Structural changes in hemoglobin during adsorption to solid surfaces: effects of pH, ionic strength and ligand binding. *Proc Natl Acad Sci* 95:12271-12276.

Höök F, Rodahl M, Brzezinski P, Kasemo B (1998b). Measurements using the quartz crystal microbalance technique: dependence of energy dissipation and saturation coverage on salt concentration. *J Coll Interf Sci* 208:63-67.

Inoue T, Cox JE, Pilliar RM, Melcher AH (1987). Effect of the surface geometry of smooth and porous-coated titanium alloy on the orientation of fibroblasts in vitro. *J Biomed Mater Res* 21:107-126.

Israelachvili J, Wennerstrom H (1996). Role of hydration and water structure in biological and colloidal interactions. *Nature* 379:219-225.

Jartoft P, Krantz M (1997). Microstructuring of titanium implant surfaces with kinoform-based laser technology (diploma thesis). Gothenburg, Sweden: Chalmers University of Technology.

Johnson CA, Lenhoff AM (1996). Adsorption of charged latex particles on mica studied by atomic force microscopy. *J Colloid Interf Sci* 179:587-599.

Kasemo B (1983). Biocompatibility of titanium implants: surface science aspects. *J Prosthet Dent* 49:832-837.

Kasemo B, Gold J (1997). Application of surface science and microlithography methods to make well defined fibers for biological evaluation. In: Correlations between in vitro and in vivo investigations in inhalation toxicology. Dungworth DL, Adler KB, Harris CC, Plopper CG, editors. ILSI Monographs, Mohr U, editor. Washington, DC: ILSI Press, pp. 182-208.

Kasemo B, Lausmaa J (1985). Metal selection and surface characteristics. In: Tissue integrated prostheses: osseointegration in clinical dentistry. Brånemark P-I, Zarb GA, Albrektsson T, editors. Chicago: *Quintessence*, pp. 99-116.

Kasemo B, Lausmaa J (1986). Surface science aspects on inorganic biomaterials. *CRC Crit Rev Biocompatibil* 2:335-380.

Kasemo B, Lausmaa J (1988). Biomaterial and implant surfaces; on the role of cleanliness, contamination and preparation procedures. *J Biomed Mater Res; Appl Biomater* 22(A2):145-158.

Keller CA, Kasemo B (1998). Surface specific kinetics of lipid vesicle adsorption measured with a quartz crystal microbalance. *Biophys J* 75:1397-1402.

Krozer A, Nordin S-A, Kasemo B (1995). Layer by layer deposition of 5-50 nm colloidal silica particles studied by quartz microbalance. *J Colloid Interf Sci* 176(2):479-484.

Kösslinger C, Uttenthaler V, Drost S, Aberl F, Wolf H, Brink G, *et al.* (1995). Comparison of the QCM and the SPR method for surface studies and immunological applications. Sensors and Actuators B-Chemical 24(1-3):107-112.

Larsson M, Ekberg M, Nikolajeff F, Hård S (1994). Successive development optimization of resist kinoforms manufactured with direct-writing, electron beam lithography. *Appl Optics* 33:1176-1179.

Lesem LB, Hirsch PM, Jordan JA Jr (1969). The kinoform: a new wavefront reconstruction device. *IBM J Res Dev* 13:150-155.

Lundström I (1985). Models of protein adsorption on solid surfaces. *Progr Coll Polym Sci* 70:76-82.

Meyle J, Gultig K, Nisch W (1995). Variation in contact guidance by human cells on a microstructured surface. *J Biomed Mater Res* 29:81-88.

Munro MS, Eberhart RC, Maki NJ, Brink BE, Fry WJ (1983). Thromboresistant alkyl derivatized polyurethanes. *ASAIO J* 6:65-75.

Nakayama Y, Matsuda T (1995). Surface microarchitectural design in biomedical applications: preparation of microporous polymer surfaces by an excimer laser ablation technique. *J Biomed Mater Res* 29:1295-1301.

Nimeri G, Fredriksson C, Elwing H, Liu L, Rodahl M, Kasemo B (1998). Neutrophil interaction with protein-coated surfaces studied by an extended quartz crystal microbalance technique. *Colloids and Surfaces B: Biointerfaces* 11:255-264.

Norde W (1996). Driving forces for protein adsorption at solid surfaces. *Macromol Symp* 103:5-18.

Persson SHM, Olofsson L, Hedberg L, Sutherland D, Olsson E (1998). A self-assembled single electron tunneling device. *Ann NY Acad Sci* 852:188-196.

Pum D, Sára M, Messner P, Sleytr UB (1991). Two-dimensional (glyco)protein crystals as patterning elements for the controlled immobilization of functional molecules. *Nanotechnology* 2:196-202.

Ratner B (1996). The engineering of biomaterials exhibiting recognition and specificity. *Molecular Recognition* 9:617-625.

Rodahl M, Höök F, Krozer A, Brzezinski P, Kasemo B (1995). Quartz crystal microbalance setup for frequency and Q factor measurements in gaseous and liquid environments. *Rev Scientif Inst* 66:3924-3930.

Rodahl M, Höök F, Fredriksson C, Keller CA, Krozer A, Brzezinski P, *et al.* (1997). Simultaneous frequency and dissipation factor QCM measurements of biomolecular adsorption and cell adhesion. *Faraday Discuss* 107:229-246.

Sackmann E (1996). Supported membranes: scientific and practical applications. *Science* 271:43-48.

Singhvi R, Stephanopoulos G, Wang DIC (1994). Review: effects of substratum morphology on cell physiology. *Biotechnol Bioeng* 43:764-771.

Tengvall P, Lundström I, Liedberg B (1998). Protein adsorption studies on model organic surfaces: an ellipsometric and infrared spectroscopic approach. *Biomaterials* 19:407-422.

Thiel PA, Madey TE (1987). The interaction of water with solid surfaces: fundamental aspects. *Surf Sci Rep* 7:211-385.

Thomas KA, Cook SD (1985). An evaluation of variables influencing implant fixation by direct bone apposition. *J Biomed Mater Res* 19:875-901.

Vogler EA (1998). Structure and reactivity of water at biomaterial surfaces. *Adv Colloid Interf Sci* 74:69-117.

Wilke HJ, Claes L, Steinemann S (1990). The influence of various titanium surfaces on the interface shear strength between implants and bone. In: Clinical implant materials. Heimke G, Soltész U, Lee AJC, editors. Advances in Biomaterials. Vol. 9. Amsterdam: Elsevier, pp. 309-314.

Wong K, Johansson S, Kasemo B (1996). Nanofabricated model catalysts: manufacturing and model studies. *Faraday Discuss* 105:237-246.

Yan SR, Fumagalli L, Dusi S, Berton G (1995). Tumor necrosis factor triggers redistribution to a Triton-X-100-insoluble, cytoskeletal fraction of β_2 integrins, NADPH oxidase components, tyrosine phosphorylated proteins, and the protein tyrosine kinase p58fgr in human neutrophils adhered to fibrinogen. *J Leukoc Biol* 58:595-606.